

AN EFFICIENT SEMI-DOUBLE-MOMENT BULK MICROPHYSICS SCHEME

Jason Milbrandt and Ron McTaggart-Cowan
Atmospheric Numerical Prediction Section, Environment Canada, Canada

1. INTRODUCTION

In atmospheric models, the interactions between hydrometeors in resolved clouds are simulated by cloud microphysics parameterization schemes. Due to the high computational cost of bin-resolving schemes, 3D models generally use bulk microphysics schemes (BMSs), in which the hydrometeor size distribution of each particle category is represented by an analytical function. Microphysical growth rates are then formulated for one or more moments of the distribution. Many BMSs employ the single-moment approach, in which there is one prognostic variable for each category proportional to the mass mixing ratio. There is a growing awareness in the modelling community of the advantages of the double-moment approach, in which the total number concentration is also a prognostic variable. However, the use of double-moment (or higher) schemes is more computationally costly due to the need to advect more prognostic variables as well as the cost of the additional predictive equations in the scheme itself. Consequently, many BMSs used in research models, and all schemes (to our knowledge) used in operational numerical weather prediction (NWP) models, are single-moment.

In this study, a new version of an existing bulk microphysics scheme is under development. The new version exploits the benefits of the double-moment approach for the hydrometeor categories to which the number of prognostic moments is most sensitive, while maintaining a relatively high level of efficiency by treating the remaining categories as single-moment. The resulting computational cost is expected to be comparable to that of a typical multi-category single-moment scheme. Despite its overall efficiency, the new scheme should be capable of simulating a wide range of meteorological conditions without the need for tuning of parameters for specific types of weather.

A description of the proposed BMS along with some preliminary results of high-resolution (2.5-km grid-spacing) NWP simulations of a mid-latitude squall line are presented. The following section provides a brief overview of the advantages of predicting more than one moment in a BMS. In section 2, we summarize the multi-moment scheme on which the modified semi-double-moment version is based. Section 4 describes the modifications for the proposed version of the scheme. In section 5, simulations are presented, showing results using the fully single-moment and fully double-moment versions of the BMS. Concluding remarks are given in section 6.

2. ADVANTAGES OF DOUBLE-MOMENT

a. Sedimentation

In order to motivate the incorporation of the double-moment approach into a scheme aimed at operational NWP, we briefly examine some important benefits of higher-moment bulk schemes. One of the most important benefits arises from the fact that in a multi-moment framework, the sedimentation is computed by allowing each of the prognostic variables to sediment at their respective moment-weighted terminal fall velocities (differential sedimentation). In double-moment (or higher) schemes, the result of this is to mimic the effects of gravitational size-sorting through a realistic redistribution in the vertical of the moments of the size spectrum.

This effect can be illustrated through simple calculations of pure sedimentation in a column, with no growth processes or interactions amongst particles. Figure 1 depicts the vertical profiles of hydrometeor mass content (top row) and mean-mass diameter (bottom row) that result from pure sedimentation of hail, with prescribed initial values at upper levels, as calculated by a single-moment bulk scheme, double-moment bulk schemes, and an analytic bin model. It is readily apparent that there is a fundamental improvement in the treatment of sedimentation for double-moment over single-moment schemes. Not only is the vertical redistribution of mass much more realistic, but also a double-moment scheme captures the effect of the redistribution of the largest mean-

Corresponding author address: Dr. Jason Milbrandt
2121 TransCanada Highway, 5th floor
Dorval, QC, H9P 1J3 Canada
e-mail: jason.milbrandt@ec.gc.ca

particle sizes towards the lower part of the profile, as in the analytic model (and nature). This is accomplished despite the fact that the entire size distribution at each level is represented by only two independent parameters. In the single-moment scheme, the mean-mass diameters (and all other moments) are directly related to the mass contents – an intrinsic limitation of the single-moment approach.

One of the problems with many double-moment schemes arises from fixing the dispersion of the hydrometeor size distribution, usually through the use of an inverse-exponential function [(i.e. with a fixed spectral dispersion parameter $\alpha=0$; see Eq. (1)]. Differential sedimentation results in uncontrolled size-sorting and excessively large mean-particle sizes and fall velocities. Milbrandt and Yau (2005a) showed that this can be controlled by allowing a variable spectral dispersion, which can be realized by either predicting a third moment (such that the dispersion is effectively an independent parameter) or by allowing the dispersion parameter to vary as a diagnostic function of the predicted moments. In the middle panels of Fig. 1, the solid [dot-dashed] lines correspond to computations from a diagnostic-dispersion [fixed-dispersion, (inverse-exponential)] double-moment scheme. The fixed-dispersion solutions exhibit excessively large mean-mass diameters and sedi-

mentation rates. In contrast, the diagnostic-dispersion approach corrects this problem.

Figure 2 depicts the surface precipitation rates that result from pure sedimentation corresponding to the sedimentation profiles shown in Fig. 1. The diagnostic-dispersion double-moment approach nearly reproduces the triple-moment calculation (not shown in Fig. 1), which is close to the analytic solution.

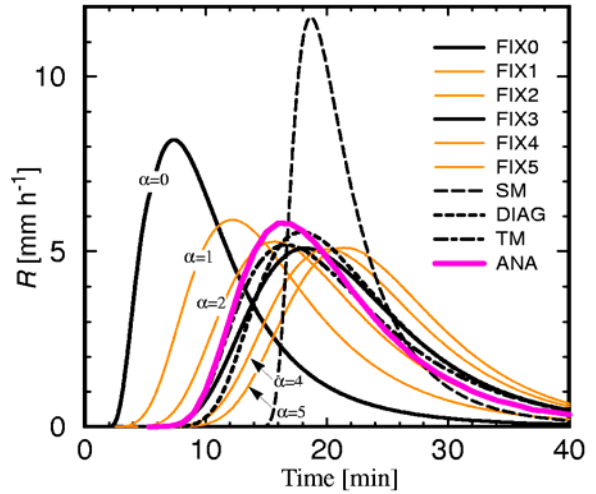


Fig. 2 Time series of surface precipitation rates from pure sedimentation computed using the indicated bulk methods. FIX(x) denotes double-moment fixed $\alpha=x$; SM denotes single-moment; DIAG denotes double-moment diagnostic-dispersion, TM denotes triple-moment; and ANA denotes the analytic solution. Reproduced from Milbrandt and Yau (2005a).

The improvements for a higher-moment BMS that result from the treatment of sedimentation are not merely aesthetic nor do they simply affect only the timing of surface precipitation. The redistribution of the moments of the size distributions subsequently results in changes in the microphysical growth rates, which in turn feed back to the dynamics through latent heating and cooling during phase changes. Further, for simulations of strong convection the location of the hydrometeor mass in a vertical column can have an important impact on the amount of precipitation loading that affects the vertical air motion.

b. Other benefits of double-moment

In addition to the direct and indirect benefits due to differential sedimentation, a scheme that independently predicts the hydrometeor mass content and total number concentration can more realistically simulate certain microphysical

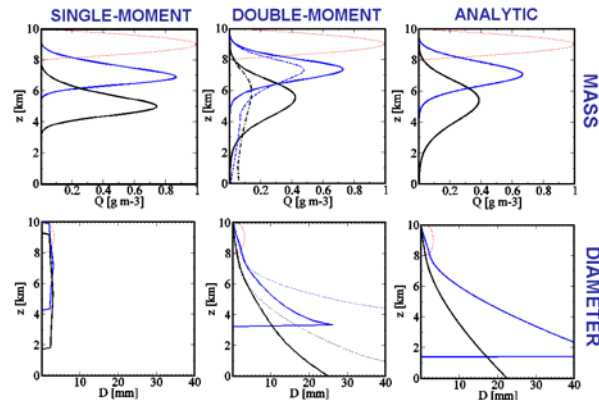


Fig. 1 Vertical profiles of hydrometeor mass content (top) and mean-mass diameter (bottom) resulting from pure sedimentation of hail with prescribed initial values at upper levels as calculated by a single-moment bulk scheme (left), double-moment bulk schemes (middle), and an analytic model (right). Profiles shown are at the initial time (red), after 4 min (blue), and after 8 min (black). For the middle panels, the solid [dot-dashed] lines correspond to computations from a diagnostic-dispersion [fixed-dispersion] double-moment approach.

processes. For example, the processes of accretion and diffusional growth affect the mass content while leaving the total number concentration constant. In contrast, aggregation and particle breakup affect the total number without changing the total mass. Thus, a double-moment scheme is better able to treat these processes than a single-moment scheme, which is constrained to have a monotonic relation between mass and number at all times.

3. ORIGINAL MICROPHYSICS SCHEME

a. Overview of scheme

The proposed semi-double-moment scheme is based on the multi-moment bulk microphysics scheme described in Milbrandt and Yau (hereafter MY, 2005a,b). A brief overview of the original scheme is provided here with a description of the proposed modifications given in the following section. The MY scheme has six hydrometeor categories – *cloud*, *rain*, *ice*, *snow*, *graupel*, and *hail*. The size distribution of each category x is represented by a gamma function of the form:

$$N_x(D) = N_{0x} D^{\alpha_x} e^{-\lambda_x D}, \quad (1)$$

where N_{0x} , λ_x , and α_x are generally referred to as the “intercept”, “slope”, and spectral dispersion (or shape) parameters, respectively, and D is the particle diameter. Spherical particles are assumed. The full version of the MY scheme is triple-moment for all categories (except *cloud*, which is double-moment), with prognostic equations for the total number concentration (N_x), mass mixing ratio (q_x), and radar reflectivity (Z_x) of each category x , corresponding to the 0th, 3rd, and 6th moments, respectively. Thus, each of the parameters in (1) varies independently. There are also single-moment (prognostic q_x only) and double-moment (prognostic q_x and N_x) options for the scheme. One double-moment version assumes a fixed value for α_x , which is the approach in nearly all published double-moment bulk schemes. The second allows for a variable spectral dispersion by incorporating a diagnostic relation for α_x as an increasing function of the mean-mass particle diameter, D_x . This approach avoids the additional computational cost of predicting three independent moments while still retaining the benefit of the controlled size-sorting.

b. Results from previous studies

The first major test of the triple-moment version of the MY scheme was published by MY (2006a) who performed a 1-km mesoscale model

simulation of a tornadic supercell. Sensitivity tests using the various versions of the scheme showed that while the diagnostic-dispersion double-moment version closely reproduced most of the important aspects of the triple-moment simulation, the fixed-dispersion simulations suffered from the problem of excessive size-sorting, exhibiting unrealistically large mean-particle sizes, reflectivities, and instantaneous precipitation rates (MY 2006b). The single-moment simulations differed from the triple-moment run in several ways, including having notably different storm structures and propagation speeds.

Milbrandt et al. (2008a,b) conducted a similar set of sensitivity tests using the MY scheme for an orographically-enhanced winter precipitation IMPROVE-2 case. In contrast to MY (2006b), there was much less variation amongst the simulations using the various versions of the schemes. This suggests that the important effects of a multi-moment scheme, at least in terms of the fields of interest for operational NWP, may be more pronounced for deep convection than for winter-type synoptically-forced weather systems.

4. SEMI-DOUBLE-MOMENT VERSION

The guiding principle in designing a new version of the MY scheme is the exploitation of the benefits of the double-moment approach with the maintenance of as much computational efficiency as possible. The goal is that the scheme be usable for operational NWP with no *a priori* assumptions about the type of weather. An important point is that not all hydrometeor categories benefit as strongly by being double-moment. Various studies have shown the importance of *hail* and *rain* being double-moment [e.g. MY (2006b)]. On the other hand, a single-moment treatment may be sufficient for categories such as *graupel*, whose range of terminal fall velocities is small.

a. General description

The size distribution of each hydrometeor category x in the semi-double-moment version is described by Eq. (1), as in the original BMS. The hydrometeor categories *cloud* and *graupel* are single-moment, with the q_c and q_g as the prognostic variables. *Rain* and *hail* are double-moment, with q_r , N_r , q_h , and N_h prognosed and the spectral shape parameters for each category (α_r and α_h) diagnosed (see section 2). There is also a new double-moment hybrid *ice-snow* category, with q_i and N_i predicted, which is described below. Table 1 summarizes the hydrometeor categories

and prognostic variables in the proposed semi-double-moment scheme.

Hydrometeor Category	Prognostic Variables	Dispersion Parameter
<i>cloud</i>	q_c	fixed ($\alpha_c = 0$)
<i>rain</i>	q_r, N_r	diagnostic α_r
<i>ice</i>	q_i, N_i	diagnostic α_i
<i>graupel</i>	q_g	fixed ($\alpha_g = 0$)
<i>hail</i>	q_h, N_h	diagnostic α_h

Table 1. Summary of hydrometeor categories in the semi-double-moment version of the MY scheme.

b. New Hybrid Ice Category

For ice crystals, we combine the previously separate categories of *ice*, representing pristine crystals, and *snow*, representing large crystals and aggregates, and introduce a double-moment hybrid *ice* category. An alternative this approach, for a similar computational cost, would be to use two separate single-moment categories, as is often done in BMSs. With this double-moment single-category approach, however, it is possible to distinguish between tiny crystals and large crystals/aggregates for a given mass content, while still permitting the simulation of the observed effects of gravitational size sorting as well as the proper representation of processes such as aggregation and diffusion (i.e. with independent tendencies of mass and total number). Morrison and Grabowski (2008) recently used a similar approach for a single hydrometeor ice-phase category (but with the added sophistication of also predicting the portion of rimed mass). Also, the fall speed parameters for our hybrid *ice* category depend on the mean-mass diameter, D_i , where parameters appropriate for small crystals (aggregates) are used if D_i is small (large).

We also include the some other changes to the treatment of the *ice* category, similar to approaches recently put forward by Thompson et al. (2008) and others. Rather than assuming the *ice* to be spherical, with an exponent $d=3$ in mass-diameter relation,

$$m(D) = c_i D^{d_i}, \quad (2)$$

and a prescribed bulk density (incorporate into c_i), as in the original MY scheme (and others) for the *ice* and *snow* categories, the new hybrid category assumes a more realistic value $d=2$, in better agreement with observed ice particles. Further, a size-dependent bulk ice density is applied, as in

Thompson et al. (2008), rather than a single fixed value.

Most microphysics schemes model diffusional growth of ice following the electrostatic capacitance analogy [e.g. Rogers and Yau (1989)]. However, recent laboratory and field research has shown that due to irregularities in the shapes of real ice crystals, the electrostatic analogy overestimates diffusional growth by a factor of 2 to 8 or more (Bailey and Hallett, 2006; Field et al. 2006). This may partly account for the excessive *snow* growth in BMSs in general. The use of experimentally determined *effective* capacitances of ice may be a way of improving simulated deposition rates. Simulations of an orographic precipitation case using the MY scheme have shown that by applying a reduction factor of 0.25 to the diffusional growth equation in the scheme results in a simulated snow mass field that more closely reproduce values of mass concentration taken by *in situ* aircraft measurements (Milbrandt et al., 2008b). In view of this, the hybrid *ice* category will also include this reduction factor in the diffusional growth term, though further testing is required to determine an appropriate value to use in general.

c. Sedimentation

The calculation of hydrometeor sedimentation is one of the most computationally expensive parts of a microphysics scheme. This is particularly so for model configurations that use large time steps (i.e. compared to time steps used in cloud resolving models, which are on the order of 1 s). The bulk fall velocity for categories such as *rain* and *hail* can result in Courant numbers (C) much greater than 1 if the full model time step were applied on a typical vertical grid increment. This necessitates the need for either time-splitting for the sedimentation calculations or the use of numerical methods that allow for stable solutions when C exceeds 1. The problem is even more severe for double-moment schemes, in which gravitational size-sorting leads to large mean-mass diameters and thus large bulk fall velocities – i.e. larger than would normally occur for a single-moment scheme. Time-splitting, in addition adding computational cost, also introduces unwanted smoothing of the hydrometeor fields due to numerical diffusion.

In the original MY scheme, an Eulerian advection scheme was used to compute sedimentation. The amount of time-splitting was determined based on a worst-case scenario – computing the sedimentation time step by

assuming the maximum allowable fall velocity and the minimum vertical grid-spacing. Though the scenario is seldom realized, this assumption was necessary to ensure vertical stability. The new scheme uses the box-Lagrangian advection method of Kato (1995) to compute sedimentation. Tests have shown that this modification dramatically improved the efficiency of the original scheme. Our experience has indicated that some amount of time-splitting is still required to avoid numerical noise. We have found that in general a maximum allowable C of 3 for sedimentation results in stable solutions. Also, an estimate of the maximum C is made in each column (for each category) at a given time step to determine the amount of time splitting that is required.

There are other possible approaches to optimizing the sedimentation calculations, such as the use of pre-computed look-up tables (e.g. Fiengold et al., 1998). We remark that while this topic may be essentially a technical issue, it is important since computational cost alone may prohibit the use of a double-moment microphysics for operational NWP, thereby removing the benefits.

d. Expected efficiency

Timing tests have indicated that runs using the 2.5-km GEM model with the optimized fully double-moment version of the MY scheme (with 12 prognostic variables) increase the total run time by approximately 18-20% compared to runs using the fully single-moment version (with 6 prognostic variables). We estimate that the increased cost of running the semi-double-moment version (with 8 prognostic variables) will be approximately 10%. Note that the increase total cost is not identical for each variable. Although the cost of advection is the same, the cost of sedimentation is greatest for the variables of categories with the fastest fall velocities. Thus, the additional cost of having *hail* double-moment, for example, is (unfortunately) greater than the cost of adding an additional single-moment category.

5. SIMULATIONS OF A SQUALL LINE

In this section, we present the case study that will be used to evaluate the performance of the proposed semi-double-moment version of the scheme. In order to establish a baseline, fully single-moment and double-moment runs are analyzed and compared. Once the modified version of the MY scheme is finalized, the results from sensitivity tests will be evaluated in the

context of the testbed developed here. We selected the 12-13 June 2002 IHOP (International H2O Project) case. During this event, thunderstorms that formed near the Oklahoma panhandle matured into a distinct squall line which passed southeastward through Oklahoma City, decaying as it approached the Oklahoma-Texas border. A squall line is an appropriate type of case for this study due to the presence of both convective and stratiform regions, each having distinctly different growth environments for microphysical fields. This is also one of the cases that will be investigated at the 2008 WMO Cloud Modeling Workshop, with the primary focus on the storm and cold pool initiation and morphology and on the ability of different models with different BMSs to develop the trailing stratiform rain region.

a. Model description

Simulations were conducted using the Canadian operational Global Environmental Multiscale (GEM) model (Côté et al. 1998). The GEM is based on the fully-compressible Euler equations and has a comprehensive physics package which includes a planetary boundary layer scheme based on turbulent kinetic energy, implicit (explicit) vertical (horizontal) diffusion, and a detailed land-surface scheme. The solar and infrared radiation package is fully interactive with the model clouds. The simulations used 58 terrain-following eta-like vertical levels. The regional configuration of the model (global, with $\Delta x \sim 15$ km over North America) was first run for a 48-h integration, initialized using the Canadian Meteorological Centre regional analysis for 0000 UTC 12 June 2002. The model was then nested to a high-resolution ($\Delta x \sim 2.5$ km) limited-area grid, centered over Oklahoma, for two 36-h integrations, one using the single-moment version of the MY scheme (SM) and the other with the double-moment (diagnostic-dispersion) version (DM) to treat grid-scale condensation. No convective parameterization scheme was used in the high-resolution runs.

b. Simulation Results

Figures 3 and 4 depict the equivalent radar reflectivity at ~ 2 km (above ground level) computed from the sum of the sixth moment of the hydrometeor size distributions from the SM and DM simulations, respectively, at 0600 UTC 13 June 2002, 24 h after the initial time of the 2.5-km runs. The corresponding observed reflectivity at 2 km from the WSI NOWRAD US mosaic is shown in Fig. 5. While the timing and location of the sim-

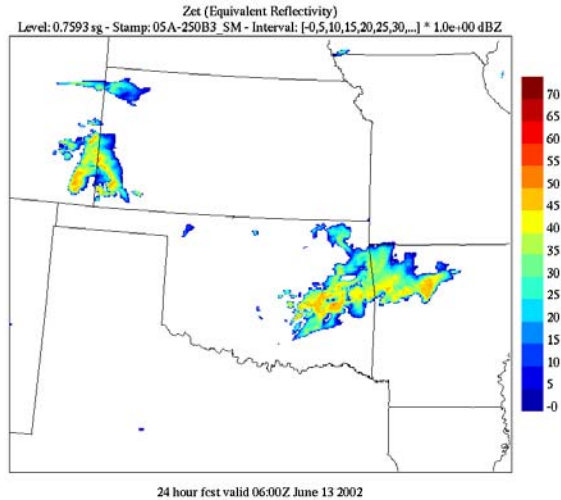


Fig. 3 Simulated reflectivity (dBZ) at ~2 km from the SM run at 13 June 0600 UTC.

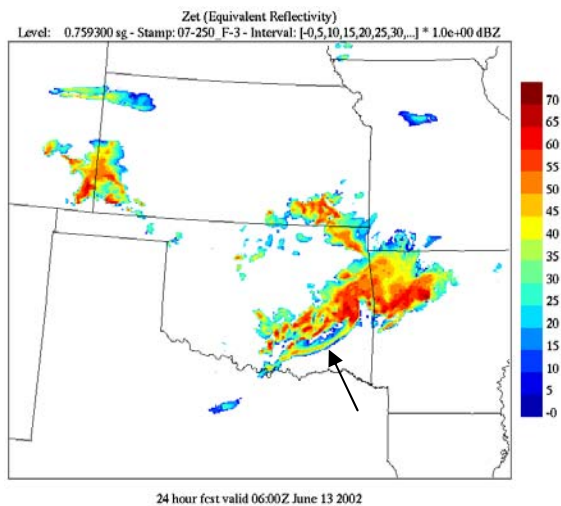


Fig. 4 As in Fig. 3 but for the DM simulation.

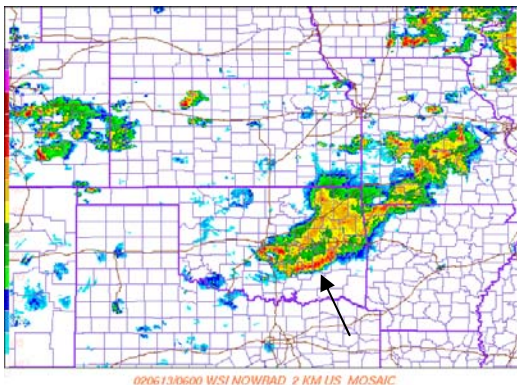


Fig. 5 Reflectivity (dBZ) at 2 km from WSI NOWRAD radar at 13 June 0600 UTC.

ulated squall lines in both runs compares well with the radar, the structures of the simulated storms are notably different. Overall, the DM simulation

compares more favorably to the observations, with a more pronounced convective band along the leading edge, particularly along the south-west portion of the system (see arrows in Figs. 4 and 5), followed by a second convective region behind this band. Note that the configuration of the two simulations is identical except for the version of the BMS. Thus, the number of prognostic moments has a distinct effect on the storm structure of the convective system, not just on the instantaneous precipitation rates (not shown).

The reason for the sensitivity of storm structure to the number of moments is due to the microphysical feedbacks of the storm dynamics. The impact of changes to the microphysics scheme on the storm dynamics can be readily seen by comparing the instantaneous fields of potential temperature (θ) from the two simulations. Figure 6 depicts the mean boundary layer (lowest 10 model levels) θ from the DM simulation along with the difference in the mean θ from DM and SM, at the time corresponding to Figs. 3-5. The most conspicuous difference is the region of colder low-level air in south-central Oklahoma, along the leading edge of the squall line in the DM simulation and observed radar. A vertical cross-section of the θ difference field, along with a 3D field of cloud mixing ratio from the DM simulation, are shown in Fig. 7. The location of the temperature differences in relation to the cloud water field strongly suggests that the colder air in south-central Oklahoma in the DM simulation is due to evaporative cooling from precipitation along the leading convective portion of the system, captured in the DM run (Fig. 4) but absent in the SM run (Fig. 3).

Potential Temperature (DM) and Difference (DM-SM) for 0600 UTC 13 June

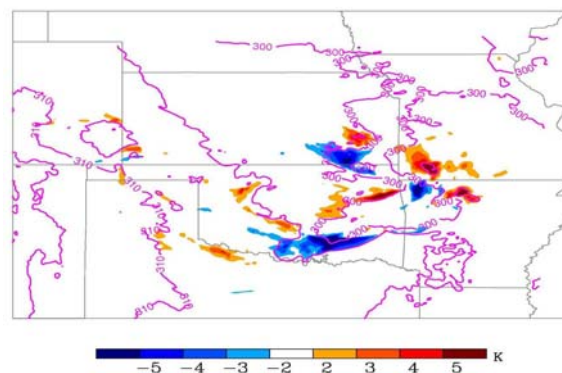


Fig. 6 Lowest model-level potential temperature from the DM simulation (purple contours, 5 K interval), valid at 13 June 0600 UTC, and the layer-averaged (lowest 10 levels) potential temperature difference field (shading) for DM-SM.

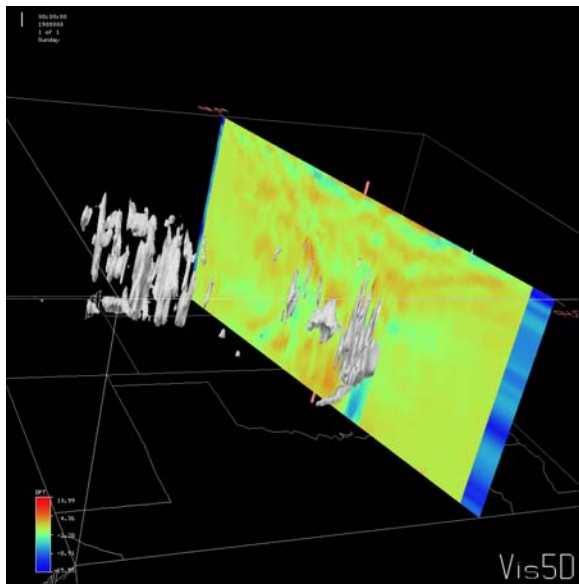


Fig. 7 Vertical cross-section of the potential temperature difference field (shading) for DM-SM and the 3D cloud water field from the DM simulation, valid at 13 June 0600 UTC.

6. CONCLUSION

An efficient semi-double-moment version of the MY multi-moment scheme is currently being developed. Some important benefits of double-moment schemes in general have been described and a description of the major modifications for the proposed scheme has been given. High-resolution simulations of the 12-13 June 2002 IHOP mid-latitude squall line using fully single-moment and double-moment versions of the BMS have been presented. The model runs illustrate that the number of moments impact on the dynamics and structure of the simulated convective system. The double-moment simulation also provides a baseline against which the semi-double-moment version will be evaluated.

For other types of cases, the effects of the microphysics can be even more pronounced, with a completely different convective mode in the simulated storm. Process studies with mesoscale models, as well as high-resolution operational NWP, would be better served with double-moment rather than single-moment BMSs, particularly for cases involving deep convection. Limitations in computational resources have, however, restricted many research and operational models to the use of single-moment schemes. In the foreseeable future, computer power will likely allow for the use of fully double-moment schemes

for all atmospheric modeling applications that use bulk schemes. In the meantime, it is important to consider schemes that are at least double-moment for the hydrometeor categories for which there is the greatest impact, thus benefiting from the double-moment approach without increasing the total run time of the models prohibitively.

Simulations of the squall line case using the semi-double-moment version of the MY scheme will be presented at the conference. The success of the proposed version of the scheme will be evaluated by comparison with observations and the double-moment simulation presented here, as well as its overall efficiency. It is planned that the semi-double-moment version will be used in the high-resolution configuration of Environment Canada's operational forecast model for the 2010 Winter Olympics in Vancouver, Canada.

REFERENCES

- Bailey, M. and J. Hallett, 2006: Measured ice crystal capacitances: The failure of the electrostatic analogy. *Proceedings, 12th Conference on Cloud Physics*, Madison, WI, 10-14 July 2006.
- Côté, J., S. Gravel, A. Méthot, A. Patoine, M. Roch, and A. Staniforth, 1998: The operation CMC-MRB Global Environmental Multiscale (GEM) model. Part I: Design considerations and formulation. *Mon. Wea. Rev.*, **126**, 1373-1395.
- Kato, T., 1995: A box-Lagrangian rain-drop scheme. *J. Meteor. Soc. Japan*, **73**, 241-245.
- Feingold, G., R.L. Walko, B. Stevens, and W.R. Cotton, 1998: Simulations of marine stratocumulus using a new microphysical parameterization. *Atmos. Res.*, **47-48**, 505-528.
- Field, P. R., A. J. Heymsfield, A. Bansemer and C. H. Twohy, 2006: Capacitance of snowflakes. *Proceedings, 12th Conference on Cloud Physics*, Madison, WI, 10-14 July 2006.
- Milbrandt, J. A. and M. K. Yau, 2005a: A multimoment bulk microphysics parameterization. Part I: Analysis of the role of the spectral shape parameter. *J. Atmos. Sci.*, **62**, 3051-3064.
- and -----, 2005b: A multimoment bulk microphysics parameterization. Part II: A proposed three-moment closure and scheme description. *J. Atmos. Sci.*, **62**, 3065-3081.

- and -----, 2006a: A multimoment bulk microphysics parameterization. Part III: Control simulation of a hailstorm. *J. Atmos. Sci. J. Atmos. Sci.*, **63**, 3114-3136.
- and -----, 2006b: A multimoment bulk microphysics parameterization. Part IV: Sensitivity experiments. *J. Atmos. Sci.*, **63**, 3137-3159.
- , -----, J. Mailhot, and S. Bélair, 2008a: Simulation of an orographic precipitation event during IMPROVE-2. Part I: Evaluation of the triple-moment run. *Mon. Wea. Rev.* (in press)
- , -----, -----,-----, and McTaggart-Cowan, R., 2008b: Simulation of an orographic precipitation event during IMPROVE-2. Part II: Sensitivity experiments. (submitted to *Mon. Wea. Rev.*)
- Rogers, R. R. and M. K. Yau, 1989: A Short Course on Cloud Physics. Pergamon, 293 pp.
- Thompson, G. P. R. Field, R. M. Rasmussen, and W. D. Hall, 2008: Explicit forecasts of winter precipitation using an improved bulk microphysics scheme. Part II: Implementation of a new snow parameterization. *Mon. Wea. Rev.* (in press).
- Morrison, H. and W. W. Grabowski, 2007: A novel approach for representing ice microphysics in models: Description and tests using a kinematic framework. *J. Atmos. Sci.* (in press).